Breakup of the conduction band structure of dilute $GaAs_{1-y}N_y$ alloys

A. Patanè, J. Endicott, J. Ibáñez,* P. N. Brunkov,† and L. Eaves
School of Physics and Astronomy, University of Nottingham, Nottingham NG7 2RD, United Kingdom

S. B. Healy, A. Lindsay, and E. P. O'Reilly
Tyndall National Institute, University College, Lee Maltings, Prospect Row, Cork, Ireland

M. Hopkinson
Department of Electronic and Electrical Engineering, University of Sheffield, S3 3JD Sheffield, United Kingdom
(Received 21 September 2004; revised manuscript received 12 January 2005; published 6 May 2005)

Using a combination of optical, electrical, and magnetotunneling measurements on resonant tunneling diodes incorporating a $GaAs_{1-y}N_y$ quantum well, we demonstrate that the conduction band states of the $GaAs_{1-y}N_y$ layer undergo a marked change with increasing N content. The abrupt change in the electronic properties of $GaAs_{1-y}N_y$ differs significantly from the smoother variation with alloy composition observed in other alloy material systems, such as $In_xGa_{1-x}As$. We show that the incorporation of N in GaAs gives rise to a qualitatively different type of alloy phenomena: N impurities and N clusters act to localize the extended Bloch states of GaAs at characteristic resonant energies, thus breaking up the energy–wave-vector dispersion relations and reducing the Γ character of the electronic states near the conduction band edge.

DOI: 10.1103/PhysRevB.71.195307 PACS number(s): 73.22.−f, 73.61.−r, 78.20.−e, 71.55.Eq

I. INTRODUCTION

In recent years, research on dilute nitride $GaAs_{1-y}N_y$ and $In_xGa_{1-x}As_{1-y}N_y$ alloys has become an active area in condensed matter physics due to the unusual physical properties of these new material systems.[1–3] The large electronegativity of the N atoms combined with the stretching and compression of neighboring bonds in $In_xGa_{1-x}As$ strongly perturbs the band structure properties of the host crystal. An important manifestation of this perturbation is the huge band gap bowing with increasing N content and a strong redshift of the band gap. These electronic properties have significant potential for several heterostructure devices such as 1.3-μm lasers, solar cells, and heterojunction bipolar transistors.[3]

Despite many years of intense research in this topical field, the electronic properties of dilute nitride alloys are still not well understood. Methods used to describe conventional alloys, such as the virtual crystal approximation, cannot be used to model these unusual material systems. Instead alternative approaches have been implemented such as the two-level band anticrossing (BAC) model,[4,5] which describes the conduction band of $In_xGa_{1-x}As_{1-y}N_y$ alloys in terms of the admixing and hybridization of the extended $In_xGa_{1-x}As$ conduction band states with the localized single N-impurity levels. On the other hand, a more complex picture has emerged from detailed band structure calculations which consider multivalley coupling[6–8] and the formation of a N-impurity band.[9] To date, none of these models succeeds in providing an exhaustive description of the unusual electronic properties revealed by experiments and reported in the current literature.[3] For example, although most of these models can describe band gap energies, none of them can account for the differing values revealed by various experimental techniques of the effective mass m_e of the conduction electrons and/or nonmonotonic dependence of m_e on y.[9–13] A clear understanding of the band structure properties has also been hindered by severe limitations on the accurate control of the electronic properties of $In_xGa_{1-x}As_{1-y}N_y$. In fact, the incorporation of N in $In_xGa_{1-x}As$ leads not only to isolated N impurities but also to the formation of N-N pairs, where a group-III atom has two N nearest neighbors, and of higher-order N clusters. The localized electronic levels of these complexes have energies below and above the conduction band minimum of the host crystal and affect strongly the electronic properties of $In_xGa_{1-x}As_{1-y}N_y$.[14–21]

In a recent experiment,[22] we have used magnetotunneling spectroscopy (MTS) experiments to probe directly the conduction band structure of $GaAs_{1-y}N_y$ at low y ($\sim$0.1%) and to demonstrate that the admixing and hybridization of the extended GaAs conduction band states with the localized single N-impurity states cause a splitting of the conduction band into highly nonparabolic hybridized subbands, thus validating the simple idea of a two-level repulsion in the BAC model.[4,5] The spatially extended nature of the $GaAs_{1-y}N_y$ conduction band states was also clearly indicated by our magnetoconductivity studies of a two-dimensional electron gas in *n*-type modulation-doped $GaAs_{1-y}N_y$/(AlGa)As quantum well (QW) heterostructures with $y=0.1\%$.[23] These revealed Shubnikov–de Haas oscillations and quantum Hall effect plateaus. These measurements indicate that the electrical conduction occurs through the extended conduction band states of $GaAs_{1-y}N_y$, albeit with relatively low mobility [$\mu=0.2\ m^2/(V\,s)$ at 4.2 K] due to scattering by N atoms.[23,24] An interesting outcome of these recent works is that at low y ($\sim$0.1%) there is a well-defined k vector for the hybridized band states of $GaAs_{1-y}N_y$ over an extended range of energy. Of particular interest is the unusual form of the lower-energy hybridized subband in which an inflection point occurs in the $\varepsilon(k)$ curve at a relatively low value of k ($\sim 4\times10^8\ m^{-1}$), considerably smaller than the size of the Brillouin zone. We suggested that this property

could be exploited to realize a new type of nonlinear device in which electrons are accelerated by an electric field up to and beyond the inflection point,[22] thus leading to a negative differential drift velocity effect, with a qualitatively different origin from that occurring in Gunn diodes[25] and superlattices.[26]

In a broader context, the combination of N doping and quantum confinement could dramatically increase the power and scope of band structure engineering as a tool for the design of a new generation of electronic devices. But to which degree can the N doping be used to tailor the conduction band? And to what extent can the two-level BAC model provide an accurate description of $GaAs_{1-y}N_y$? To answer these questions, in this paper we examine in detail how the electronic properties of $GaAs_{1-y}N_y$ evolve with increasing N content. To probe the energy and wave vector, and also the character (i.e., whether impurity like or band like) of the N-induced states, we use a combination of magnetotunneling, capacitance-voltage, and optical spectroscopy measurements on a series of tunneling diodes, which incorporate a $GaAs_{1-y}N_y$ QW layer. The measurements reveal that these electronic properties change rapidly with increasing y. For low N composition ($y \sim 0.1\%$), the form of the measured $\varepsilon(k)$ dispersion relations of the N-induced subbands can be understood in terms of a simple two-level BAC model involving isolated N atoms. However, we also find that the Γ character of the N-induced states depends on energy and k vector. As the N content increases up to about 0.2%, N clustering tends to reduce further the Γ character of the electronic states and to break up the energy–wave-vector dispersion relations. Our data and analysis using the linear combination of isolated nitrogen states (LCINS) model[27] reveal an abrupt change in the electronic properties of $GaAs_{1-y}N_y$ with increasing y, due to N clustering. This behavior differs significantly from the smoother variation with varying alloy composition observed in other alloy material systems, such as $In_xGa_{1-x}As$, for which the k vector, the $\varepsilon(k)$ dispersion relations, and the effective mass values remain well defined over the whole range of In composition.

II. RESONANT TUNNELING DIODES CONTAINING DILUTE NITRIDES

Our samples were grown by molecular beam epitaxy on (100)-orientated n-type GaAs substrates. In the first set of structures, a 8-nm-wide $GaAs_{1-y}N_y$ ($y=0$, 0.08%, 0.43%, 0.93%, 1.55%) QW layer is embedded between two 6-nm $Al_{0.4}Ga_{0.6}As$ tunnel barriers. In the second set of samples $y=0.20\%$ and the $GaAs_{1-y}N_y$ layer has a width of 7 and 10 nm. In all samples, undoped GaAs spacer layers, each of width 50 nm, separate the $Al_{0.4}Ga_{0.6}As$ barriers from n-doped GaAs layers in which the doping concentration is increased from 2×10^{17} cm^{-3}, close to the barrier, to 2×10^{18} cm^{-3}. The thicknesses of these two n-doped GaAs layers are 50 nm and 500 nm, respectively, in the outer layers of the "sandwich" structure. The samples were processed into circular mesas with diameters between 25 and 400 μm, with a ring-shaped top contact to allow optical access for current-voltage $I(V)$ measurements under illumination and for photoluminescence (PL) and photocurrent (PC) studies. For the PL measurements, the diode was excited with a He-Ne laser. The PL was dispersed by a 0.5-m monochromator and detected by an (InGa)As detector. The excitation source for the PC measurements was a He-Ne laser or a tungsten-halogen lamp, dispersed by a 0.25-m monochromator. The PC signal was recorded using standard lock-in techniques. Capacitance-voltage $C(V)$ measurements were made with an HP 4275A LCR meter over the frequency range from 10 kHz to 1 MHz.

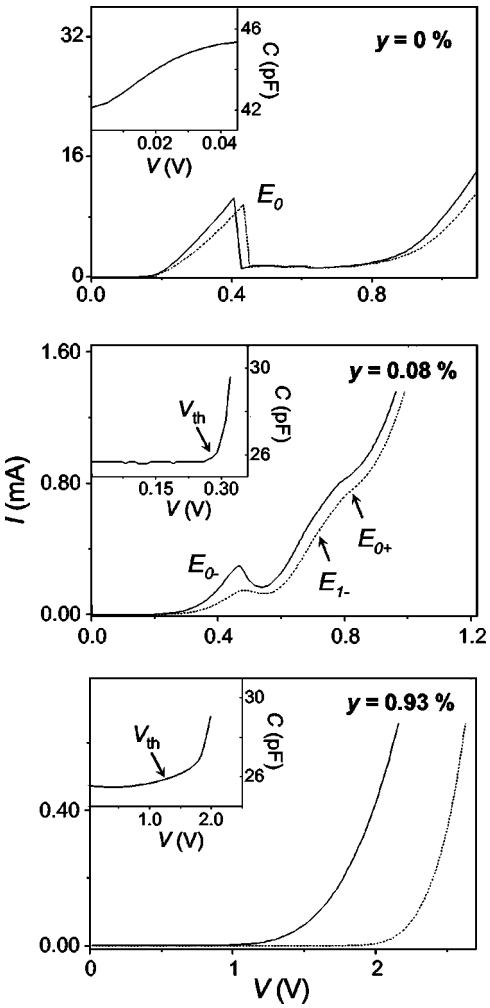

FIG. 1. $I(V)$ curves at 10 K in the dark (dotted lines) and under illumination (solid line) for $GaAs_{1-y}N_y$ QW's with $y=0\%$, 0.08%, and 0.93%. Each sample was excited with above-band-gap laser light (633 nm) and power densities of about 10 W/cm^2. Insets show $C(V)$ curves. The arrows indicate the threshold voltage V_{th} for increase of capacitance.

As shown in Fig. 1, when we compare the $I(V)$ curves of the control sample ($y=0\%$) and of the sample with $y=0.08\%$, we find that the resonant peak E_0 due to electrons tunneling through the lowest-energy quasibound subband of the QW is replaced by three features E_{0-}, E_{1-}, and E_{0+} associated with electron tunneling into the three lowest-energy subbands of the $GaAs_{1-y}N_y$ QW. They arise from hybridization of the unperturbed host-matrix QW subbands E_0 and E_1 with the localized N-resonant state. Around $k=0$, subbands

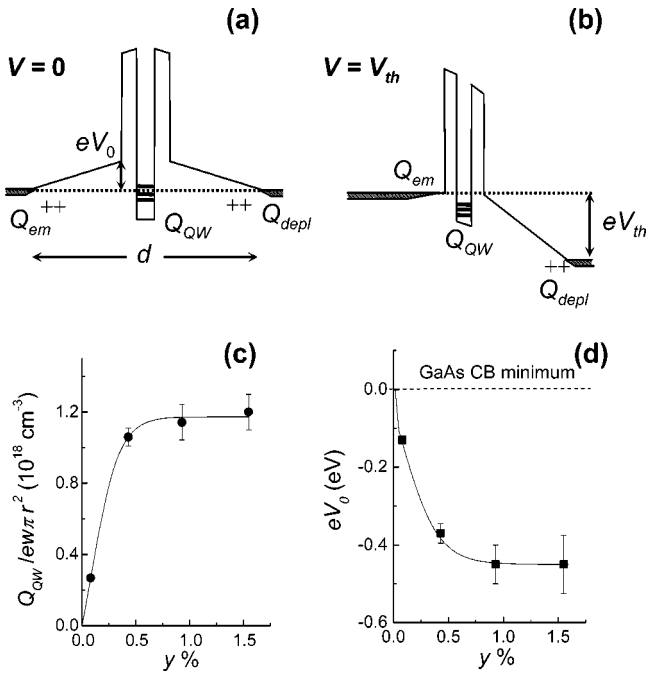

FIG. 2. (a), (b) Schematic diagrams of the conduction band profile for our tunneling diodes for $V=0$ and $V=V_{th}$. (c), (d) y dependence of the volume density of electrons trapped in the well, $Q_{QW}/e\pi wr^2$, and of the average energy position eV_0 of the N-trap levels as measured with respect to the GaAs CB minimum.

E_{0-} and E_{1-} exhibit a dominant bandlike character, while E_{0+} has a significant impurity-N-like nature.[22] Clear resonant features in $I(V)$ were also observed in tunneling diodes with $y=0.2\%$ and different well widths ($w=7$ and 10 nm). In contrast, a further increase of y strongly quenches the current and shifts to higher biases the threshold voltage at which the current increases rapidly. Under excitation with light, the current flow is increased; in particular, the resonant features in the $I(V)$ curve of the sample with $y=0.08\%$ are strongly enhanced (see Fig. 1). These changes induced by increasing y are accompanied by variations in the capacitance-voltage curves $C(V)$ (see insets of Fig. 1). In the control sample ($y=0$), the capacitance of the diode rises at a relatively low bias. In contrast, the $C(V)$ curves of samples with $y>0\%$ show an almost constant capacitance ($\sim$26 pF) over an extended voltage range between zero bias and a threshold voltage V_{th}.

The marked change in the $I(V)$ and $C(V)$ curves at large y suggests that N incorporation has profound effects on the electron tunneling dynamics and the charge distribution. The disappearance of the resonances in $I(V)$ for samples with large y ($y=0.43\%$, 0.93%, and 1.55%) indicates an increasing amount of disorder in the well. The disorder breaks the condition for conservation of the in-plane wave vector, which is required to observe a well-defined peak in $I(V)$ for electron tunneling into an energy-dispersed subband. Also the strong suppression of current and the threshold voltage V_{th} in the $C(V)$ curves of samples with $y>0$ suggest the existence of a significant number of N-related electron traps in the $GaAs_{1-y}N_y$ layer. As shown schematically in Fig. 2(a), at zero bias, equilibrium is established by electrons diffusing from the doped GaAs layers into the lowest-energy levels of the $GaAs_{1-y}N_y$ QW layer. The resulting negative charge in the well gives rise to two depletion layers in the regions beyond the $Al_{0.4}Ga_{0.6}As$ barriers and to a relatively wide region of dielectric, which is depleted of free carriers.[28] Therefore, a significant applied voltage V_{th} is required to reach flatband conditions on the emitter side of the device and hence lead to an increase of the capacitance and tunneling current [see Fig. 2(b)]. Note that the increase of capacitance induced by the increasing applied voltage becomes less sharp at high N concentrations. This suggests that increasing y leads to a broader energy distribution for the electron traps.[19]

Using Poisson's equation for our resonant tunneling diodes (RTD's), we model the $C(V)$ data and extract the average energy position and density of the electron traps in the QW that lie below the Fermi energy in the n-doped GaAs emitter layer. The capacitance is defined as $C=dQ/dV$, where $dQ=-dQ_{em}-dQ_{QW}=dQ_{dep}$ is the incremental change of the charge in the emitter layer (dQ_{em}) and in the QW (dQ_{QW}) for an incremental change in the applied voltage, dV. The corresponding increase in the positive charge in the collector depletion layer is dQ_{dep}.[29] Assuming that the negative charge in the QW layer (Q_{QW}) does not change between $V=0$ and $V=V_{th}$, then the value of Q_{QW} is determined using the relation $\int_0^{V_{th}} CdV = C_0V_{th} = \int_0^{V_{th}} dQ_{depl} = Q_{QW}/2$, where C_0 is the constant value of capacitance measured for $V<V_{th}$. Using the experimental values of C_0 and V_{th}, we estimate that the volume density of electrons trapped in the well is $Q_{QW}/e\pi wr^2 = 2C_0V_{th}/e\pi wr^2 = 2.6\times10^{17}$ cm^{-3}, 1.0×10^{18} cm^{-3}, 1.1×10^{18} cm^{-3}, and 1.2×10^{18} cm^{-3} for samples with $y=0.08\%$, 0.43%, 0.93%, and 1.55%, respectively, where $r=100$ μm is the radius of the mesa and $w=8$ nm is the well width. Figure 2(c) shows the increase of charged electron traps with increasing y as deduced from the $C(V)$ curves. The density of traps is much smaller than that of isolated N atoms, which varies from 1.8×10^{19} cm^{-3} for $y=0.08\%$ to 3.4×10^{20} cm^{-3} for $y=1.55\%$. We estimate that the electron traps are located at an energy given by $eV_0=eV_{th}/2$ below the GaAs conduction band minimum.

We find that eV_0 is equal to about 0.1 eV and 0.4 eV for $y=0.08\%$ and $y>0.08\%$, respectively [see Fig. 2(d)], although the determination of V_{th}, and hence of V_0, becomes less accurate at high y [see vertical bar in Fig. 2(d)]. These values are larger than those reported for N-N pairs in previous works for samples with smaller N content ($y<0.1\%$).[15,19,20] However, note that higher N concentrations may favor the formation of N clusters and N-related defects with deeper energy levels. For $y\sim0.1\%$, our data are similar to those measured by optical techniques in Refs. 16 and 17. These works report binding energies in the range 0.04–0.16 eV. For $y>0.1\%$, our data also support previous studies showing the existence of deep N-related defects, attributed in those studies to nitrogen-split interstitial defects.[30,31]

Electron trapping on N-related localized states also accounts for the strong photoinduced current enhancement observed in all RTD's with $y>0\%$ (see Fig. 1 for $y=0.08\%$ and 0.93%). Figure 3 shows the dependence on the light excita-

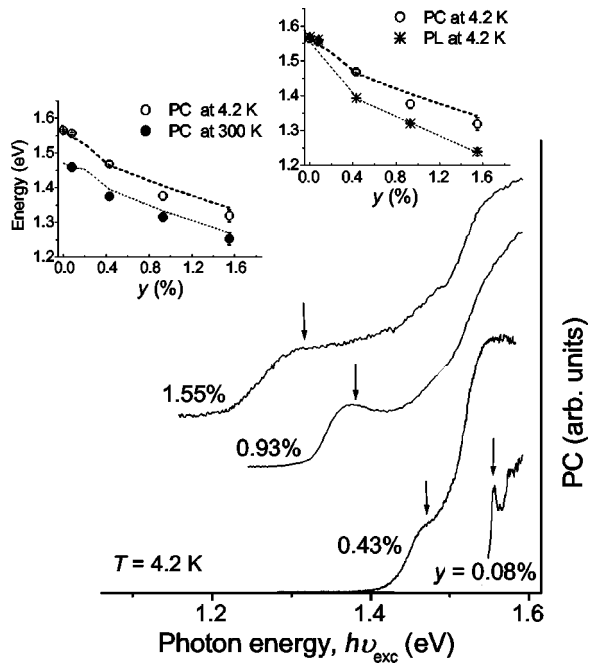

FIG. 3. PC spectra at 4.2 K. The vertical arrow indicates the energy peak position of the N-related PC band. Left inset: energy peak position of the N-related PC band at 4.2 K and 300 K. The lines show the y dependence of the band edge absorption energy of $GaAs_{1-y}N_y$ at 4.2 K and 300 K according to the LCINS model. Right inset: energy peak position of the N-related PC and PL bands at 4.2 K. The lines are guides to the eye.

tion energy, $h\upsilon_{exc}$, of the intensity of the PC signal measured under applied bias corresponding to electron and hole tunneling into the $GaAs_{1-y}N_y$ QW layer. Similar plots were obtained for different excitation power and/or applied biases. The form of the spectra is weakly affected by the applied bias, although the intensity is bias dependent because of the effect of the bias on the number and energy of electrons and holes tunneling into the QW. The low-temperature (T =4.2 K) PC spectra of all structures show a current enhancement for $h\upsilon_{exc} > 1.5$ eV, which arises from carriers photocreated in the GaAs layers on each side of the barriers and QW.[32] The PC spectra also reveal a weaker band that shifts to lower energy when the amount of N is increased (see vertical arrow in Fig. 3). We assign this to the effect on the tunnel current of carriers photocreated across the band gap of the $GaAs_{1-y}N_y$ QW layer: the direct photoexcitation of carriers in the QW and subsequent hole recombination with electrons on the localized charged N-induced states in the well leads to an increased number of electrons tunneling into and out of the well.[33] The intensity of the corresponding photoinduced current depends on the interband optical absorption of the $GaAs_{1-y}N_y$ QW layer and provides us with a means of investigating how the band gap absorption of the $GaAs_{1-y}N_y$ QW changes with increasing y. We find that the N-related PC band due to the exitonic absorption in the QW shifts in energy and broadens considerably with increasing N content. Electrons and holes injected and/or photocreated in the $GaAs_{1-y}N_y$ QW layer also recombine to produce a strong PL signal. Our low-temperature (T=4.2 K) PL spectra show that the N-related PL emission is redshifted relative to the corresponding PC band and that the redshift, referred to as the Stokes shift, increases significantly when y is increased from 0.1% to about 0.4% (see inset of Fig. 3).

III. BREAKUP OF THE CONDUCTION BAND STRUCTURE AT HIGH y

The disappearance of the resonances in $I(V)$, the increase in the number of electron traps revealed by the $C(V)$ data, and the significant energy broadening of the optical lines for increasing y shown in Figs. 1–3 respectively, indicate that the $GaAs_{1-y}N_y$ QW layer undergoes a significant change in character with increasing N content. This behavior, which differs from the smoother dependence with varying alloy composition observed in other alloy material systems, such as (InGa)As and (AlGa)As, indicate an unusual and marked transition of the electronic properties from band like to strongly disordered at high y.

To probe in more detail the electronic properties $GaAs_{1-y}N_y$, we use magnetotunneling spectroscopy (MTS). Our resonant tunneling and optical spectroscopy experiments at zero magnetic field described in the previous section allow us to probe the bound states of the $GaAs_{1-y}N_y$ QW layer around $k=0$, but they do not provide the k dependence of the energies of the QW subband states. In a MTS experiment, a magnetic field B is applied perpendicular to the current direction. Varying the intensity of B allows us to tune an electron to tunnel into a given k state of the well; the voltage tunes the energy so that by measuring the voltage position of the resonances in $I(V)$ as a function of B, we can map out the $\varepsilon(k)$ dispersion relations of $GaAs_{1-y}N_y$.[22]

Figure 4(a) shows grey-scale contour plots of the value of the differential conductance $G=dI/dV$ as a function of energy and wave vector derived from a simple analysis of the MTS measurements for two QW's, one with $y=0.08\%$ and $w=8$ nm and the other with $y=0.2\%$ and $w=10$ nm. The white-stripe-like regions in the plots of Fig. 4(a) correspond to minima of G just beyond the resonant peak in the $I(V)$ curves. The minimum in the negative differential conductance associated with each resonance allows us to track accurately how the voltage position and amplitude of the resonances vary with increasing B. To reveal clearly how each resonance evolves with increasing B, we also plot in Fig. 4(a) a narrow range of G. Plots of the peak of G show similar dependence on magnetic field, although less clearly due to the resonance broadening caused by charging of the well.[34]

The $\varepsilon(k)$ curves reveal energy regions of anticrossing [indicated by horizontal arrows in Fig. 4(a)] and indicate that the localized states associated with N impurities and N—N pairs admix and hybridize with the subband states of the QW, thus breaking up the conduction band at characteristic resonant energies. The brightness and width of these stripes provides information about the character, impurity like or band like, of the states in the $GaAs_{1-y}N_y$ QW. The hybridization between the Γ conduction band states and the localized N and N-N pair energy levels gives the N-related states of the $GaAs_{1-y}N_y$ QW a partly Γ character over a wide energy range and allows electrons to tunnel into them from the

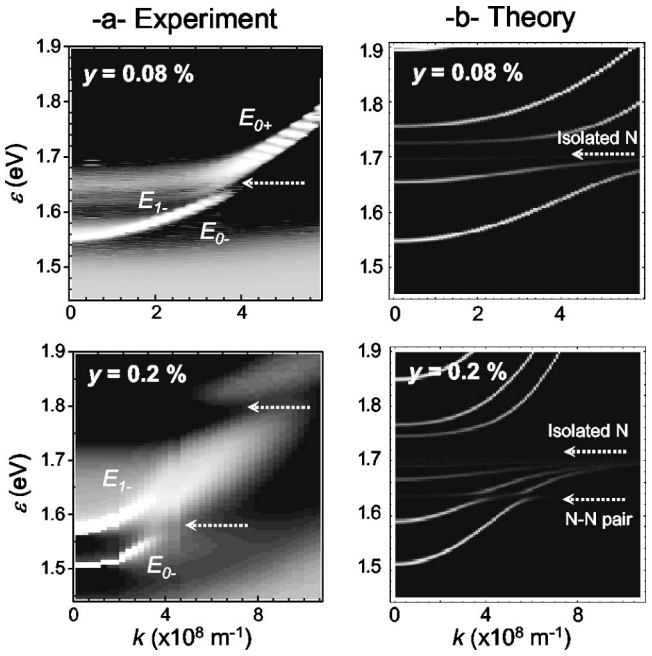

FIG. 4. (a) Grey-scale plots of the differential conductance G vs ε and k as derived from MTS measurements for $y=0.08\%$ and 0.2%. The bright stripes correspond to regions of low G. The energy position of the lowest subband E_{0-} at $k=0$ is derived from the measured energy position of the N-related PC band at 4.2 K and is plotted relative to the top of the valence band. (b) Three-level BAC model calculations of the contour plots of the fractional Γ character f_Γ of the hybridized $GaAs_{1-y}N_y$ QW subbands vs ε and k for $y=0.08\%$ and 0.2%. The bright sections of the plot correspond to increasing values of the fractional Γ character f_Γ.

GaAs emitter accumulation layer, where the band states have a pure Γ character. At ε and k values for which the Γ character of the QW states is very small, electron resonant tunneling from the emitter is negligible, so no negative differential conductance occurs; these regions appear as black on the grey-scale plots of Fig. 4(a).

Using this analysis, the partial Γ character of the hybridized states of the $GaAs_{1-y}N_y$ QW can be "tagged" by magnetotunneling spectroscopy. In Fig. 4(a), for $y=0.08\%$, the weakening of the E_{0-} and E_{1-} resonances at large k is consistent with the strongly localized character of the lowest hybridized subband states of the $GaAs_{1-y}N_y$ QW layer at energies close to those of isolated N impurities; in contrast, the strong enhancement of the E_{0+} resonance at large k and the corresponding increase of the energy–wave-vector dispersion indicate that with increasing k, the E_{0+} subband states become more delocalized in real space, i.e., they acquire an increasing Γ character. For $y=0.2\%$, the $\varepsilon(k)$ curves reveal two energy regions of anticrossing at around 1.6 eV and 1.8 eV. We believe that for this sample, the subband states of the QW admix and hybridize not just with isolated N impurities, but also with the localized energy states associated with N-N pairs that are resonant with the conduction band states of GaAs. This further breaks up the $\varepsilon(k)$ dispersion relations. In Fig. 4(a) and at $y=0.2\%$, the weakening of the E_{0-} resonance at energies of about 1.6 eV and 1.8 eV and corresponding wave vectors $k\sim 4\times 10^8$ m^{-1} and 8×10^8 m^{-1} [see horizontal arrows in Fig. 4(a)] indicates that the lowest hybridized subband states of the $GaAs_{1-y}N_y$ QW layer become increasingly localized as they approach the energy of isolated N impurities ($\sim$1.7 eV) and N-N pairs ($\sim$1.6 eV). This effect is not clearly resolved for the second E_{1-} resonance, which tends to quench and merge with the E_{0-} resonance for increasing voltages (energies) and magnetic fields (k vectors).

For $y>0.2\%$, the measured $G(V)$ curves show no resonances and are almost unaffected by magnetic fields up to the available field of 14 T. In this case, it is likely that the isolated N impurities and N clusters break the translational symmetry required for a well-defined k vector and $\varepsilon(k)$ dispersion relations in the QW.

IV. DISCUSSION: FROM THE ULTRADILUTE ($y\sim 0.1\%$) TO THE DILUTE REGIME ($y>0.1\%$)

In our previous works,[22,23] we have demonstrated that for y up to $\sim$0.1% there is a well-defined k vector for the hybridized conduction band states of $GaAs_{1-y}N_y$ over an extended range of energy and that the simple idea of a two-level repulsion in the BAC model provides a qualitative description of the form of the energy dispersion curves measured by magnetotunneling spectroscopy.[22] However, the BAC model does not include the effect on the band structure of N-N pairs and N clusters. These effects are clearly revealed by experiment[7,15–21] and also suggested by detailed band structure calculations of $GaAs_{1-y}N_y$.[6–8] Neither the detailed theoretical calculations nor the BAC model provide a description of the measured $\varepsilon(k)$ dispersion relations and/or account for the marked and unusual transition in the optical and transport properties of $GaAs_{1-y}N_y$ discussed in the previous sections.

In an attempt to explain these data, we extend the BAC model to include the interaction between the GaAs host conduction band Γ states and the full range of N-related levels in the alloy, with the N states described explicitly using a LCINS model.[27] The model is based on detailed tight-binding (TB) calculations of the energy levels of isolated N impurities, N-N pairs, and N clusters, including the strength of their interaction with the host matrix Γ states. Using the tight-binding method, we calculate explicitly a distribution of energy levels that is generally similar to that found in Refs. 6 and 18. We then calculate the influence of this distribution of states on the conduction band edge and on higher-lying levels. Comparison with full TB calculations confirms that the conduction band of $GaAs_{1-y}N_y$ is indeed well described in terms of interactions between the GaAs conduction band Γ states and this LCINS, distributed at random in an ultralarge supercell.[27,35] The LCINS model allows us to describe in detail how the electronic properties of $GaAs_{1-y}N_y$ are affected by a random distribution of N isolated impurities and clusters at different values of y.

The interaction between the different N states and the GaAs extended conduction band edge Γ state reduces the fractional Γ character f_Γ of the lowest conduction band level in $GaAs_{1-y}N_y$. This effect is already well known from the two-level BAC model,[5] as illustrated by the solid line in Fig.

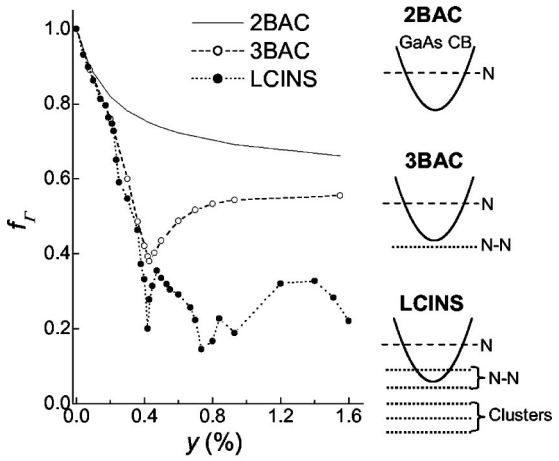

FIG. 5. Fractional Γ character f_Γ of the CB minimum of a $GaAs_{1-y}N_y$ QW with well width $w=8$ nm and different y according to the two-level BAC, three-level BAC, and LCINS models. The insets sketch the CB of GaAs and the energy levels of N impurities, N-N pairs, and higher-order N clusters.

5. We also show in Fig. 5 the calculated value of f_Γ using two other models: (i) the LCINS model and (ii) a three-level BAC model,[36] which accounts for the hybridization of the GaAs Γ conduction band states with isolated N states and N-N first-neighbor [110] pairs.[37]

For $y<0.2\%$, the values of f_Γ calculated using the different models are indistinguishable. This indicates that at low y, N clustering has very little effect on the conduction band edge. This is not unexpected as the density of N-N pairs and of more complex N clusters arising from a random incorporation of N is small for $y\sim0.1\%$ ($\sim10^{17}$ cm^{-3}) and much smaller than the density of isolated N atoms ($\sim10^{19}$ cm^{-3}). Each N atom has 12 nearest neighbors on the group-V sublattice. The probability of one of these neighbors being a N atom in a random alloy is $12y$ for small y, so that we expect the number of N-N pairs will grow as $6y^2$. The number of larger N clusters will start to grow more slowly with y, e.g., initially as $\sim y^3$ for clusters where three N atoms are linked to each other via common Ga neighbors. Since the confinement energy of the QW pushes the conduction band minimum above the energy levels associated with the small number of N-N first-neighbor [110] pairs (~1.5 eV) and N clusters (<1.5 eV), N clustering plays a minor role at low y.[36] In contrast, as shown in Fig. 5, for $y>0.2\%$ the values of f_Γ calculated within the two-level BAC model (which ignores clustering) become larger than those estimated within the three-level BAC and LCINS models and indicate that N clustering acts to reduce significantly the Γ character of the conduction band edge at large y. The band edge value of f_Γ for $y\sim0.4\%$ (see data points) is associated with the anticrossing and hybridization between the conduction band edge and the energy level at about 1.5 eV associated with N-N first-neighbor [110] pairs. The value of f_Γ then recovers both for the LCINS and three-level BAC models for a further small increase of y, because the interaction with isolated N levels pushes the Γ conduction band minimum below the N-N level. At still higher values of y ($0.4\%<y<0.8\%$) the conduction band edge approaches the energy levels (<1.5 eV) associated with higher-order N clusters. For $y>0.4\%$, the divergence of the three-level BAC model (including N-N pairs) and the LCINS model (including all N clusters) reflects the increased disruption of the conduction band edge due to the higher-order N clusters.

The LCINS model describes well the energy position of the band edge absorption of the $GaAs_{1-y}N_y$ QW layer measured at different temperatures by PC for all values of y (see inset of Fig. 3). The strong reduction of f_Γ and the inhomogeneous broadening of the conduction band states caused by the random incorporation of N account for the disappearance of the resonant features in $I(V)$ when the N content is increased above about 0.2%. It also explains the unusually rapid increase in the value of the Stokes shift and energy broadening of the optical lines observed in our samples (see Fig. 3) and similar $GaAs_{1-y}N_y$ layers reported in the recent literature for $y>0.1\%$.[3,7,38]

Various models have been used in the literature[4–9] to describe successfully the energy gap of $GaAs_{1-y}N_y$, so the agreement between our data and the LCINS model shown in Fig. 3 does not represent a stringent test to validate our model. We note, however, that the LCINS model also provides a qualitatively good description of the measured $\varepsilon(k)$ curves. Figure 4(b) shows the calculated energy dispersion relations for $y=0.08\%$ and 0.2%. In these plots, the brightness of the lines increases with the fractional Γ character f_Γ of the N-induced subbands. Our calculations indicate that for low values of y, up to about 0.1%, N-N pairs and other N clusters have very little effect on the form of the energy dispersion relations, which are dominated by the effect of hybridization of the band states with isolated N impurities. The $\varepsilon(k)$ dispersions calculated using the LCINS model for y up to about 0.1% are virtually indistinguishable from those calculated using the two-level BAC model, which considers the strongly admixed character of the states, but neglects N-clustering effects. This is due to the relatively low density of N-N pairs and N clusters at these low values of y. In contrast, for a further increase of y, N-N pairs produce significant changes in the conduction band structure.

For $y=0.2\%$, we find that most of the interaction arises from states which lie close to the isolated N-resonant energy level at ~1.7 eV. However, an additional weak interaction is found at about 1.5 eV and 1.6 eV due to the interaction of band states with N-N first-neighbor [110] pairs and second-neighbor [220] pairs, respectively.[35] The first-neighbor [110] pair energy level is too far below the conduction band edge to have any significant interaction with states at 1.6 eV, whereas our calculations locate the second-neighbor [220] pair level between the lowest confined QW state and the isolated N level. As shown in Fig. 4(b) the effect of N-N pair states are clearly observed in the $\varepsilon(k)$ dispersion curves for $y=0.2\%$. The $\varepsilon(k)$ curves reveal two distinct energy regions of anticrossing indicated by horizontal arrows in Fig. 4(b). In addition to the N impurities, the localized states associated with the N-N [220] pairs at around 1.63 eV admix and hybridize with the subband states of the QW, thus disrupting the conduction band at characteristic values of energy and k vector close to those derived from the MTS measurements.

The calculated energy level for the [220] pair disagrees with the bound energy level calculated in Refs. 6 and 18.

However, we also note that there is little agreement between the various models for the energies of other N-N pairs and N clusters. The calculations in Ref. 6 include one energy state, due to the [200] pair, in the relevant energy range ($\sim$1.6 eV). However, this [200] state has opposite amplitude on the two N atoms and should therefore have close to zero interaction with the GaAs Γ states. It is therefore unlikely to cause significant disruption of the band dispersion. With these points in mind, we believe that our overall interpretation of the experimental data is correct, although the particular N-N pair responsible for the disruption of the band structure is not completely certain.

Although our model calculations shown in Fig. 4(b) predict the existence of a number of subbands with significant Γ character, we can only resolve those with low energies in the grey-scale plots of our MTS data. This is likely to be due to the rapid increase of the transmission coefficient through the barriers at the large bias voltages required for electrons tunnelling into higher-energy states of the QW, which in turn leads to broadening and weakening of the resonant features in $G(V)$ and to a very large and positive value of G.

For $y>0.2\%$, the LCINS calculations show that states associated with N-N pairs and N clusters further perturb the band dispersion at higher N content. In particular, the strong reduction of Γ character of the electronic states induced by N clustering shown in Fig. 5 indicates that an increasing range of k vectors is required to describe the electronic states at high y. This broadening effect is also observed in the measured $\varepsilon(k)$ curves of the sample with $y=0.2\%$ for which the resonances in $G(V)$ and corresponding $\varepsilon(k)$ curves show a larger energy and k-vector broadening compared to that observed in the sample with $y=0.08\%$. The isolated N impurities and N clusters act to break the translational symmetry required for a well-defined k vector and $\varepsilon(k)$ dispersion relations, leading to strong disorder and localization of the energy states. We believe that for high values of y new approaches are necessary to fully understand and interpret the optical and transport properties of dilute nitrides and also to explain some contradicting results reported in the literature concerning the electron effective mass at high values of y.[9–13] We emphasize that our data show clearly that the concept of effective mass remains valid at N contents as high as 0.2%. The curvature of the measured $\varepsilon(k)$ curves in Fig. 4(a) indicates that the electron effective mass m_e at the conduction band minimum increases from $m_e=(0.07\pm0.01)m_0$ to $(0.08\pm0.01)m_0$ as y is increased from 0.08% to 0.2%, where m_0 is the electron mass in vacuum. This albeit small increase is consistent with that calculated using our model ($m_e=0.075m_0$ and $0.079m_0$ for $y=0.08\%$ and 0.2%, respectively).

V. CONCLUSION

In conclusion, we have shown that the optical and transport properties of RTD's incorporating a $GaAs_{1-y}N_y$ QW layer between (AlGa)As barriers undergo a rapid change with increasing N content due to N clustering. For low-N compositions ($y\sim0.1\%$), the form of the energy dispersion of the N-induced subbands can be understood in terms of a two-level BAC model involving only isolated N atoms. We have also shown that the Γ character of the states depends strongly on energy and is strongly reduced at the energy of the isolated N-impurity level. As the N content increases, it becomes necessary to treat explicitly the effects of N-N pairs and/or larger N clusters on the electronic properties. Our data and analysis using the LCINS model reveal an abrupt change in the electronic properties of $GaAs_{1-y}N_y$ with increasing y. Isolated N atoms, N-N pairs, and higher-order clusters tend to reduce further the Γ character of the electronic states and break up the energy-wave-vector dispersion relations even at values of y as low as 0.2%. Clustering effects account for the disappearance of resonant features in $I(V)$ and for the rapid enhancement of disorder and localization, which are manifest in both optical and transport properties for $y>0.1\%$.

Our data reveal an abrupt change in the electronic properties of $GaAs_{1-y}N_y$, which differs significantly from the smoother variation with alloy composition observed in other alloy material systems, such as $In_xGa_{1-x}As$, for which the k vector, the $\varepsilon(k)$ dispersion relations, and the effective mass values remain well defined over the whole range of In composition. The incorporation of N in GaAs gives rise to a qualitatively different type of alloy behavior: N impurities and N clusters act to disrupt the extended Bloch states of the GaAs conduction band at characteristic resonant energies, thus leading to a duality of bandlike and electron localization phenomena and strongly modified energy dispersion curves. Remarkably, this alloy material system that has emerged as a candidate for long-wavelength optoelectronic applications due to its giant band gap bowing is now revealing a number of unique electronic properties. A comprehensive and detailed understanding of how the unusual and unique conduction band of $GaAs_{1-y}N_y$ will influence the optical and transport properties of this material system remains a challenge. New theoretical approaches and concepts such as the LCINS model used here are necessary to fully understand and exploit the remarkable electronic properties of dilute nitrides and other similar highly mismatched alloys reported in the recent literature.[39]

ACKNOWLEDGMENTS

This work is supported by the Engineering and Physical Sciences Research Council (United Kingdom), by the Spanish Ministry of Science and Technology under CICYT Project No. MAT 2001-1878 and the Ramon y Cajal program, and by Science Foundation Ireland. We acknowledge G. Hill and R. Airey for processing our samples and M. Capizzi and A. Zunger for useful discussions.

*Permanent address: Institut Jaume Almera, CSIC, Barcelona, Spain.
†Permanent address: A.F. Ioffe Physico-Technical Institute, Polytechnicheskaya 26, 194021, St. Petersburg, Russia.
[1] M. Kondow, K. Uomi, A. Niwa, T. Kitatani, S. Watahiki, and Y. Yazawa, Jpn. J. Appl. Phys., Part 1 **35**, 1273 (1996).
[2] M. Weyers, M. Sato, and H. Ando, Jpn. J. Appl. Phys., Part 2 **31**, L853 (1992).
[3] Special issues: *III-N-V Semiconductor Alloys* [Semicond. Sci. Technol. **17**, 1 (2002)] and *Dilute Nitrides* [J. Phys.: Condens. Matter **16**, 1 (2004)].
[4] W. Shan, W. Walukiewicz, J. W. Ager III, E. E. Haller, J. F. Geisz, D. J. Friedman, J. M. Olson, and S. R. Kurtz, Phys. Rev. Lett. **82**, 1221 (1999).
[5] A. Lindsay and E. P. O'Reilly, Solid State Commun. **112**, 443 (1999).
[6] P. R. C. Kent and A. Zunger, Phys. Rev. B **64**, 115208 (2001).
[7] Y. Zhang, B. Fuegel, M. C. Hanna, J. F. Geisz, L. W. Wang, and A. Mascarenhas, Phys. Status Solidi B **240**, 396 (2003).
[8] L-W. Wang, Phys. Rev. Lett. **88**, 256402 (2002).
[9] Y. Zhang, A. Mascarenhas, H. P. Xin, and C. W. Tu, Phys. Rev. B **61**, 7479 (2000).
[10] P. N. Hai, W. M. Chen, I. A. Buyanova, H. P. Xin, and C. W. Tu, Appl. Phys. Lett. **77**, 1843 (2000).
[11] D. L. Young, J. F. Geisz, and T. J. Coutts, Appl. Phys. Lett. **82**, 1236 (2003).
[12] Y. J. Wang, X. Wei, Y. Zhang, A. Mascarenhas, H. P. Xin, Y. G. Hong, and C. W. Tu, Appl. Phys. Lett. **82**, 4453 (2003).
[13] F. Masia, A. Polimeni, G. Baldassarri Höger von Högersthal, M. Bissiri, M. Capizzi, P. J. Klar, and W. Stolz, Appl. Phys. Lett. **82**, 4474 (2003).
[14] D. J. Wolford, J. A. Bradley, K. Fry, and J. Thompson, in *Proceedings of the 17th International Conference on the Physics of Semiconductors*, edited by J. D. Chadi and W. A. Harrison (Springer-Verlag, New York, 1984), p. 627.
[15] X. Liu, M. E. Pistol, L. Samuelson, S. Schwetlick, and W. Seifert, Appl. Phys. Lett. **56**, 1451 (1990).
[16] T. Makimoto, H. Saito, T. Nishida, and N. Kobayashi, Appl. Phys. Lett. **70**, 2984 (1997).
[17] S. Francoeur, S. A. Nikishin, C. Jin, Y. Qiu, and H. Temkin, Appl. Phys. Lett. **75**, 1538 (1999).
[18] Y. Zhang and A. Mascarenhas, Phys. Rev. B **61**, 15 562 (2000).
[19] Y. Zhang, A. Mascarenhas, J. F. Geisz, H. P. Xin, and C. W. Tu, Phys. Rev. B **63**, 085205 (2001).
[20] Y. J. Wang, X. Wei, Y. Zhang, A. Mascarenhas, H. P. Xin, Y. G. Hong, and C. W. Tu, Appl. Phys. Lett. **82**, 4453 (2003).
[21] Y. Zhang, B. Fluegel, M. C. Hanna, A. Mascarenhas, L. W. Wang, Y. J. Wang, and X. Wei, Phys. Rev. B **68**, 075210 (2003).
[22] J. Endicott, A. Patanè, J. Ibanez, L. Eaves, M. Bissiri, M. Hopkinson, R. Airey, and G. Hill, Phys. Rev. Lett. **91**, 126802 (2003).
[23] D. Fowler, O. Makarovsky, A. Patanè, L. Eaves, L. Geelhaar, and H. Riechert, Phys. Rev. B **69**, 153305 (2004).
[24] S. Fahy and E. P. O'Reilly, Appl. Phys. Lett. **83**, 3731 (2003).
[25] J. B. Gunn, Solid State Commun. **1**, 88 (1963).
[26] L. Esaki and R. Tsu, IBM J. Res. Dev. **14**, 61 (1970).
[27] A. Lindsay and E. P. O'Reilly, Phys. Rev. Lett. **93**, 196402 (2004).
[28] We model the diode as the series of two parallel-plate capacitors, one for the QW-emitter region and the other for the QW-collector region. The total capacitance of the diode is given by $C=\varepsilon_0\varepsilon_r A/d$, where ε_0 is the permittivity constant in vacuum, ε_r is the relative permittivity of GaAs, A is the area of the mesa, and d is the distance between the fronts of the free carrier regions on the emitter and collector sides of the device. From the value of the capacitance at zero bias, we estimate that $d=140$ nm, in good agreement with the doping profile and layer structure of our samples.
[29] E. F. Schubert, F. Capasso, A. L. Hutchinson, S. Sen, and A. C. Gossard, Appl. Phys. Lett. **57**, 2820 (1990).
[30] S. B. Zhang and S. H. Wei, Phys. Rev. Lett. **86**, 1789 (2001).
[31] P. Krispin, S. G. Spruytte, J. S. Harris, and K. H. Ploog, Appl. Phys. Lett. **80**, 2120 (2002).
[32] M. S. Skolnick, P. E. Simmonds, D. G. Hayes, A. W. Higgs, G. W. Smith, A. D. Pitt, C. R. Whitehouse, H. J. Hutchinson, C. R. H. White, L. Eaves, M. Henini, and O. H. Hughes, Phys. Rev. B **42**, 3069 (1990).
[33] A. Patanè, J. Endicott, J. Ibanez, and L. Eaves, J. Phys.: Condens. Matter **16**, S3171 (2004).
[34] M. L. Leadbeater, E. S. Alves, F. W. Sheard, L. Eaves, M. Henini, O. H. Hughes, and G. A. Toombs, J. Phys.: Condens. Matter **1**, 10 605 (1989).
[35] E. P. O'Reilly, A. Lindsay, and S. Fahy, J. Phys.: Condens. Matter **16**, S3257 (2004).
[36] S. B. Healy, A. Lindsay, and E. P. O'Reilly, IEE Proc.-J: Optoelectron. **151**, 397 (2004).
[37] When a Ga atom has two N neighbors, we refer here to the N atoms as "nearest neighbors" on the N sublattice (i.e., [110] N-N pair). Likewise, we say "second neighbors" when N atoms are linked as N-Ga-As-Ga-N (i.e., [220] N-N pair).
[38] G. Bentoumi, V. Timoshevskii, N. Madini, M. Cote, R. Leonelli, J. N. Beaudry, P. Desjardins, and R. A. Masut, Phys. Rev. B **70**, 035315 (2004).
[39] K. M. Yu, W. Walukiewicz, J. Wu, W. Shan, J. W. Beeman, M. A. Scarpulla, O. D. Dubon, and P. Becla, Phys. Rev. Lett. **91**, 246403 (2003).